

## Assessing Cyclonic Wave Heights In The Arabian Sea Using Deep Learning Models.

Susmita Biswas<sup>1\*</sup>, Debdutta Mandal<sup>2</sup>

<sup>1\*</sup>Department of Cyber Science & Technology, Brainware University, Kolkata 700125. email: bi.susmita@gmail.com.  
Tel: 91+ 9477058253

<sup>2</sup>Department of Cyber Science & Technology, Brainware University, Kolkata 700125.

Submission date-20.09.2023

Revised date-08.12.2023

Acceptance date-14.12.2023

---

### Abstract

Ocean wave heights in the Arabian Sea during tropical cyclones (TC) are predicted using deep learning models based on long short-term memory (LSTM) and bidirectional short-term memory (BLSTM) networks. The models utilize different lead times. Combining the BLSTM model with the traditional numerical wave models can provide a more accurate and computationally efficient forecast method for large wave height data. Two grids, G1 (71.5°E, 22.0°N) and G2 (67.1°E, 22.6°N), have been selected for the Arabian Sea (AS). Based on these grids, the model estimated significant wave heights are constructed, and the cyclones TAUKTAE (15 May–19 May 2021) and BIPARJOY (06 June–15 June 2023) went through. Deep learning models are used to estimate significant wave heights under severe situations, and the accuracy is compared using root mean square error (RMSE). Time series for grid G1 are examined from 1983 to 2021, whereas shorter time series for grid G2 are examined from 2013 to 2023. With the goal of achieving the least amount of error, the LSTM and BLSTM models are evaluated using various hidden units and epoch settings after being trained with 80% data. Less error was produced by the larger time-series for the training set, whether or not the TC conditions were included. The shorter time-series including the cyclonic data produced higher error for the 20% testing set. Additional forecasts with varying lead periods or delays were made, which increased inaccuracy. This has to do with the model's diminishing power as the forecast horizon gets longer.

**Keywords:** Deep learning; prediction; time series; tropical cyclones; wave heights.

### 1 Introduction

High wind speeds during the summer monsoon cause high wave heights due to the wave environment of the eastern Arabian Sea (Amrutha and Sanil Kumar 2017). The number of tropical cyclones in the Arabian Sea (AS) has increased in recent years as a result of rising sea surface temperatures increasing the frequency and strength of these storms. Research shows that the wave fields on the surface of the water during tropical cyclones are more asymmetric than the wind fields (Zhang and Oey 2019). The extended fetch of the ocean waves exists to the right of the storm center, which causes the wave fields' spatial distribution to deviate from that of the associated wind fields. The tropical storm wave spectrum's complex geographical distribution makes prediction more challenging. For the third generation of spectral ocean wave models to accurately represent the asymmetry of the ocean fields during a tropical storm, more accurate parameterizations are required. This research proposes a deep learning architecture with different lead times to forecast ocean wave heights during normal and cyclonic periods, based on long short-term memory (LSTM) network and bidirectional short-term memory (BLSTM) network. In order to reasonably anticipate Indian Ocean wind speed data, Biswas and Sinha (2021) carry out a similar investigation. As researchers experiment with high temporal and low spatial resolution data, time-series analysis is widely employed in these studies (Petitjeana et al. 2014). According to (Reddy and Prasad 2018), a time-series offers superior analysis over other data sets since it includes any transient changes comprising data from a certain time period. Time-series wave height parameter data from the AS's TAUKTAE and BIPARJOY cyclones are used in this study. Numerous deterministic model types have been developed and applied for significant wave height prediction in both normal and exceptional scenarios. In order to anticipate important wave height time-series in the Jakarta Bay, auto regressive moving average (ARIMA) models are employed (M. Alif R. Yonanta et.al. 2018). These models forecast the values in the time-series data by using the contiguous data. The parametric models are not appropriate for accurate time-series predictions since they presume linear and stable data (Reddy and Prasad 2018). With a big data set and prolonged prediction intervals of around a week, the neural network also seems to be effective in deep ocean wave forecasting. The average impact of space and time area may be to blame for this (Deo et al. 2001). Based on the most recent wave observation at a place, the neural network methodology combines complementary and straightforward methods for real-time wave prediction at a spot (Deo and Naidu 1999). The ultimate conclusion reached was that employing global learning algorithms over local learning algorithms is not beneficial (Samanta et al. 2006). An artificial neural network (ANN) is a type of information system that connects several common neurons to replicate the functions of biological neuron networks. Neurons execute basic computations using specified nonlinear functions to provide output after receiving input from one or more sources. According to (Gopinatha and Dwarakishb 2015), there are two different kinds of artificial neural

networks (ANNs): feed forward and recurrent. Recurrent neural networks (RNNs) are characterized by the presence of at least one feedback link, which allows for looping activity (Abhigna et al. 2016). A unique class of RNN model is the LSTM model, which is based on deep learning. For better wind speed prediction, ANN-based multivariate models are suggested that consider a number of characteristics, including temperature, pressure, and wind speed (Filik and Filik 2017). To get greater accuracy, deep learning algorithms often need a lot of training data. Large volumes of data are produced by wave forecasting and ocean remote sensing applications, and these data are directly linked to the real wave parameters (Wu et al. 2019). Another study uses a hybrid model of wavelet and neural network to anticipate wind waves with different lead periods (Oh and Suh 2018). Recurrent networks have a very lengthy learning curve and retain data for a very long time through repeated backups. This is largely because of insufficient flow and corrosive mistakes. However, the most widely used methods for determining the contents of short-term memory are either too slow or perform poorly altogether, particularly in cases when there is a lengthy minimum period between the input and the matching instructor signal (Hochreiter and Schmidhuber 1997). For rotating neural networks, several LSTM architectural variations have been proposed. According to (Greff et al. 2017), recursive neural networks with long short-term memory, or LSTM for short, have become scalable and successful models for a variety of learning issues involving sequential input. According to Patel et al. (2018), LSTM is a network design that effectively extracts both transient characteristics and long-term relationships from historical data. One-time step forward values can be estimated by training an LSTM network. Bidirectional long-term dependency between time-series or sequence data may be found using the BLSTM model. Algorithms for machine and deep learning are examples of outbound methods for gradually resolving prediction issues. It has been demonstrated that these methods yield more accurate findings than traditional regression-based modeling. Additional training is made possible by bidirectional LSTMs (BLSTMs), which traverse input data both forward and backward (Siami-Namini et al. 2019). Because it ignores the peculiarities of the domains, multivariate time-series data analysis and prediction has difficulties in a variety of fields. BLSTM model based on multi-time time-series data that considers the unique properties of many domains has been suggested. It uses a BLSTM model to forecast a different form of pre-processed multivariate time-series input data. In order to learn, these models primarily combine all the data from several areas (Kim and Moon 2019). Deep learning is an excellent technique that may be applied to reverse and non-linear function fitting in addition to classification. Deep survey technology has been used to execute significant wave height data evolution from real sea surface backscattering coefficient training data sets in order to replicate genuine radar detection and application of retrograde technology (Wu et al. 2019). To estimate the amount of electrical power generated by a wave energy converter, an integrated deep learning network that combines the principal component analysis (PCA) approach with the LSTM algorithm is employed. In comparison to the LSTM model alone and other machine learning models, the integrated data driven model's findings demonstrate exceptional performance (Ni et al. 2019). The trained projected deep learning model's performance is independent of the number of training cycles (Namini et al. 2018). Ocean wave conditions are predicted via a machine learning framework. Accurate representations of major wave heights and times may be utilized to forecast ocean conditions by supervised training of machine learning models on many thousands of iterations of a physics-based wave model (Jamesa et al. 2017). The latest advancements in deep learning-based computer vision have served as inspiration for the CNN-PCA approach. PCA models may easily post-process a convolution neural network (CNN) once it has been trained as an evident transformation function (Liu et al. 2019). In order to forecast SWH in the Atlantic Ocean, a unique method based on EMD modal decomposition is presented by (Zhuxinet al. 2024). The ongoing global climate change has a significant influence on the waters. Ocean waves are intricate systems that are influenced by swells and wind waves. Every year, hundreds of people die and millions more people are affected by natural catastrophes globally. One of the natural calamities that happens regularly around the world is the storm. These have an immediate influence on people's life, frequently ruin their social, biological, and physical environments, and have long-term implications for their survival, well-being, and general health. For everyone who lives close to the seaside, knowing the wave height parameter forecast during a storm is crucial to their protection. For coastal engineering and disaster management operations, one of the most significant phenomena is the forecasting of wave height. Recent years have seen a major improvement in the use of soft computing approaches for significant wave height prediction. Apart from conventional wave height prediction, a novel approach to significant wave height prediction has been investigated using soft computing approaches (Akhil and Deka 2017). Many operations on the coast and in open waters depend on the ability to predict wind wave characteristics across varying lead durations. The complexity and uncertainty of wave generation and dissipation processes are partially explained by deterministic equations, which are the foundation of numerical wave models, which normally offer this information (Makarynsky et al. 2005). In order to organize different operations related tasks at sea, sea level height forecasts are required, including a few hours or days of alert time. The differential equation that represents the wave energy balance has presently been numerically calculated to extract this information. Significant quantities of meteorological and oceanographic data are required for the highly complex solution procedure (Deo and Naidu 1999). It is hard to predict the wave conditions connected to a specific storm because of the complicated wave generation process in cyclones. Many important wave height prediction models have been produced using various methods. Comparing the benefits and drawbacks of several wave forecasting models is done by SWAMP (1985). It is challenging to predict the wave conditions connected to a specific storm due to the complex wave generation process in cyclones (Kumar et al. 2003). According to (Ali and Prasad 2019), data-intelligent algorithms that can accurately forecast the height of coastal

waves in a short amount of time in coastal regions might produce valuable insights for boosting the output of renewable energy. Third-generation spectral ocean wave models such as WAVEWATCH III (Tolman 1991) are often used to provide realistic predictions of ocean waves during cyclones. These models incorporate wind wave propagation, production, and dissipation at different depths. According to (Singh et al. 2001), a cyclone is among the most destructive natural disasters on the planet. Two cyclones from the AS region—TAUKTAE and BIPARJOY—are the focus of this investigation. Extremely Powerful Typhonic Storm from May 11 to May 19, 2021, TAUKTAE devastated areas of Maharashtra, Karnataka, and Gujarat. It originated in the Arabian Sea and was the first cyclonic storm of 2021. Areas around Kerala's coast and in Lakshadweep saw flash floods and severe rainfall due to TAUKTAE. There have also been reports of intense rainfall in the states of Maharashtra, Karnataka, and Goa. Unforgiving Cyclonic Storm in June 2023, BIPARJOY, the strongest storm in the AS region, made landfall in Maharashtra on the western coast of the state. On June 6, 2023, Cyclone Biparjoy—an Extremely Severe Cyclonic Storm—formed in the east central Arabian Sea. The system was upgraded to a cyclonic storm on June 2nd by the India Meteorological Department (IMD), and given the name BIPARJOY. The following day, BIPARJOY strengthened into a powerful cyclonic storm and veered northeast, eventually reaching landfall around 170 km of Gujrat. In this work, the cyclonic ocean wave heights for various lead periods are estimated using the LSTM and BLSTM models for the first time, and the forecast accuracy is evaluated using root mean square error analysis. The study's originality is in its use of deep learning models to estimate the important wave height parameter in real time during cyclonic circumstances. The appendix A contains the LSTM and BLSTM algorithms.

## 2 Data and Methodology

The fifth generation of atmospheric reanalysis data from the European Centre for Medium-Range Weather Forecasts (ECMWF) at a spatial resolution of 50 km is taken into consideration in this study, which consists of hourly data estimations. Important wave height data are collected and analyzed for the two grid sites in the AS areas (71.5°E, 22.0°N) and G2 (67.1°E, 22.6°N), over which the BIPARJOY and TAUKTAE cyclones passed. Data from 1983 to 2021 are considered for the TAUKTAE cyclone grid 06, 12, 18, and 24 hours, while data from 2013 and 2023 are included for the BIPARJOY grid. The time series data related to the TAUKTAE cyclone is referred to as the long time series data, while the time series data related to the BIPARJOY cyclone is referred to as the short time series data. With the time-series data mentioned above, four different experiments are carried out. The cyclonic data is first excluded, and then it is incorporated for the two cyclones that were previously discussed. Using a deep learning method, LSTM and BLSTM models are trained to estimate the wave height parameter in the two AS area grid points. In this sense, the models are developed using 06 hourly wave height data as input variables. Using the supplied wave data, two types of deep learning models (LSTM and BLSTM) have been trained. Twenty percent of the data set is used for testing, while the remaining eighty percent is used to train the models. Evaluation is done on how well the two distinct models performed during the training and testing phases. The BLSTM model outperformed the traditional LSTM model in terms of accuracy when it came to forecasting both cyclonic and non-cyclonic wave heights. Data with and without TAUKTAE period and data with and without BIPARJOY period are the two types of time series data sets utilized for each model. Subsequently, the more accurate BLSTM model is used to predict for various lead times: 1, 2, 3, 4, 8, 12; these correspond to 06, 12, 18, 24, 48, and 72 hours (H), respectively. Model performance is assessed and measured using the mean square error (MSE) and root mean square error (RMSE).

### Pseudocode of LSTM and BLSTM deep models

1. Significant wave height time series data was selected as the input data.
2. The choice of deep network architecture
3. Training and testing data were separated and further standardized.
4. The learning rate (0.005) was specified at a fixed value in the model design.
5. Choosing settings such the time step, epoch, and hidden unit.
6. To get the optimum performance, experiments based on different hidden layers were carried out.
7. The number of hidden layers was set at 250 for LSTM and 250 for BLSTM based on the aforementioned studies.
8. To get the optimal performance, several epoch values were investigated.
- 9 The deep model underwent training in order to get the lowest error performance.
10. MSE and RMSE values were used to evaluate the performance of the model.
11. MSE and RMSE values were used to evaluate the performance of the model.

#### 4 Results and Discussions

Deep learning algorithms are used to estimate the next instantaneous wave height forecast based on current and past data. In order to anticipate the important wave height data that are usually dominated by deep learning models in the AS area, the current research is an exploratory study. The wave height data for cyclonic and non-cyclonic time-series data for two distinct AS grids (71.5°E, 22°N) and G2 (67.1°E, 22.6°N) in which TAUKTAE and BIPARJOY cyclones traveled, respectively, are predicted using LSTM and BLSTM models. Time-series data from the TAUKTAE grid (long length) from 1983 to 2021 and the BIPARJOY grid (short length) from 2013 to 2023 are used in both models.

The data sets include points for 38 years, 39 years, 10 years, and 11 years, respectively, for 55520 (1983-2020), 56980 (1983-2021), 14608 (2013-2022), and 15336 (2013-2023) years. The data spanning 38 and 10 years indicates the non-cyclonic phases, while the remaining two (39 and 11 years) relate to the eras that encompassed cyclones. The time-series plots for the AS region's TAUKTAE and BIPARJOY grids are displayed in Figs. 1a and 1b. The graphic accurately captures the highest elevation of almost 6 meters during the TAUKTAE cyclone. On May 19, 2021, at 06 hours, the major wave height for the selected grid (71.5° E and 22.0° N) was 6.5 meters. On June 15, 2023, during a period of 12 hours, the major wave height for the BIPARJOY grid was 4.2 meters. Analysis and discussion of the performance of the LSTM and BLSTM models for a range of inputs have been conducted. Significant wave height data are also predicted using the BLSTM model for a range of lead times, 1, 2, 3, 4, 8, 12 (equivalent to 06, 12, 18, 24, 48, and 72 hours). LSTM and BLSTM models are used in separate experiments for the given time-series. The time series data are split into training and testing sets (20% and 80%, respectively). The current investigation tests several epochs and hidden units. For the corresponding time-series data, 250 hidden nodes and a 0.005 starting run rate are selected while considering the LSTM network model. The ideal number of epochs for the long length time-series for the periods 1983–2020 and 1983–2021 in the LSTM model is determined to be 1000 for this cutting-edge network model. It is discovered to be 2500 for the short length time-series covering the years 2013–2022 and 2013–2023. These produced more accurate findings. The ideal values for the BLSTM models are found to be 250, 250 for the hidden units and 500 and 1000 for the epochs, respectively, for the long and short length time-series data, by adjusting the number of two hidden units and epochs. There are several experiment settings ready. First, a lengthy growth curve from 1983 to 2023 is predicted by testing and training. To lessen the bias resulting from random initialization, training and testing are conducted many times. Meanwhile, RMSE is used for quantitative assessment and comparison. The residuals, or discrepancies, between the observed and expected values are calculated. The time-series prediction results for different wave heights are compared in terms of RMSE and graph visualization. Using the LSTM model for the TAUKTAE grid, Fig. 2 compares the training anticipated and training observed outcome. After the cyclonic data was included, the RMSE value went from 0.07 to 0.3 meters. Similar comparisons for the BIPARJOY grid using the LSTM model are shown in Fig. 3.

When the cyclonic data was included, the inaccuracy for the short time series rose from 0.12 to 0.26 meters. Figure 4 presents the comparisons for the TAUKTAE grid training set using the BLSTM model, whereas Figure 5 presents the same comparisons for the BIPARJOY grid. With the BLSTM model, the errors for the cyclonic data sets decreased dramatically. The LSTM and BLSTM models are then applied to the testing data sets. The contrast between testing observed data and predicted data using the LSTM model for the TAUKTAE and BIPARJOY grids, respectively, is shown in Figs. 6 and 7. The inaccuracy rose from 0.1 to 0.3 meters for both grids with the testing data set when the cyclonic wave heights were included.

Similar comparisons and error analysis using the BLSTM model are presented in Figures 8 and 9. The error is higher for the short time series than the long one, albeit being smaller than for the LSTM model. Therefore, it is reasonable to use deep learning models to forecast important wave height data under both normal and cyclonic situations.

The wave height is accurately predicted in a subsequent experiment using the BLSTM model on the four time series data provided, with lead times of 1, 2, 3, 4, 8, and 12 corresponding to 06, 12, 18, 24, 48, and 72 hours, respectively. For some operating plans, advance forecasting is helpful, and the signature of notable variations in wave height is crucial. The BLSTM model was used to assess the forecast for the next 72 hours using delay (1, 2, 3, 4, 8, and 12) and epoch 1000 for long length time-series and epoch 2500 for short length time-series. It is apparent that these models become less accurate with longer lead periods. The variations between the measured and anticipated values, as determined by BLSTM, become more apparent as lead time increases. Nonetheless, the BLSTM model still does a fair job of capturing the broad trends of the wave height fluctuations. Furthermore, variations between the observed and projected wave height time series using the BLSTM model may be readily observed when the lead time approaches 12 (72 hours). It is evident that the changes get larger as the lead time increases. The RMSE values calculated for the training data sets using the LSTM model for the AS grids are shown in Table 1. With the training data sets and the BLSTM model, Table 2 provides comparable RMSE values. Tables 3 and 4 present the testing data sets' outcomes. The tables include the hidden units for each time-series data set and the RMSE values for the various epochs. Bold text indicates the minimal error levels. The RMSE values utilizing the BLSTM model for various lead times are provided in Tables 5 and 6. These values apply to both training and testing data sets. The longer the lag time, the slower the performance gets. Including the heights of cyclonic waves, the error for

the training set for the 72-hour prediction period is 0.3 meters for the long data set and 0.4 meters for the short data set. The error for the short time-series grew significantly for the testing set. As a result, the errors are shown in the plots and tables for each model and time series data set. In every instance, the BLTM model outperformed the LSTM model in terms of accuracy.

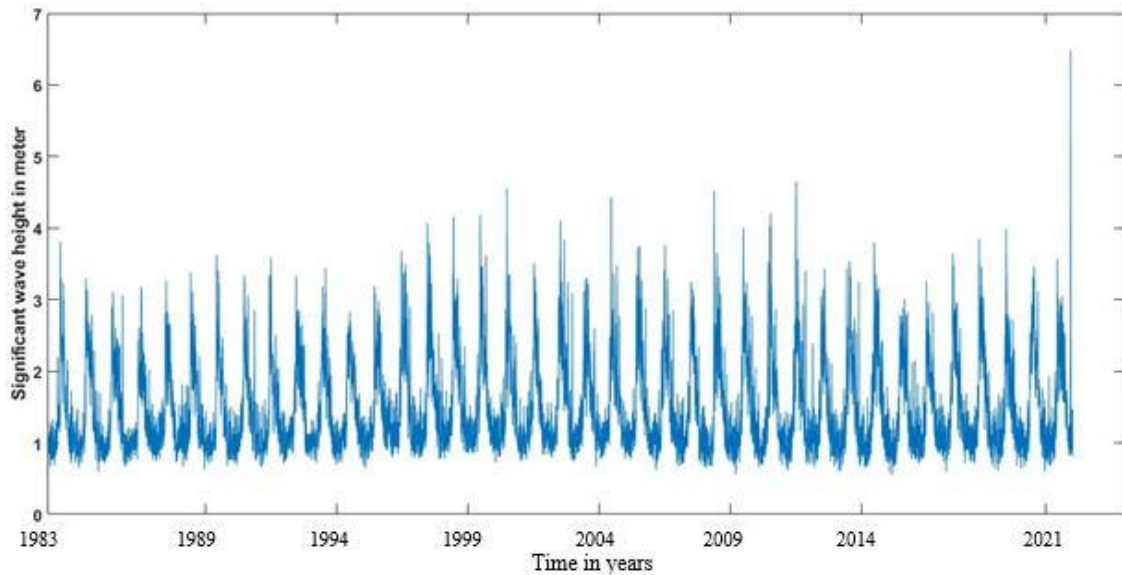


**Fig. 1a.**ERA5 significant wave height of AS (71.5°E, 22°N) grid (TAUKTAE) from 1983-2021

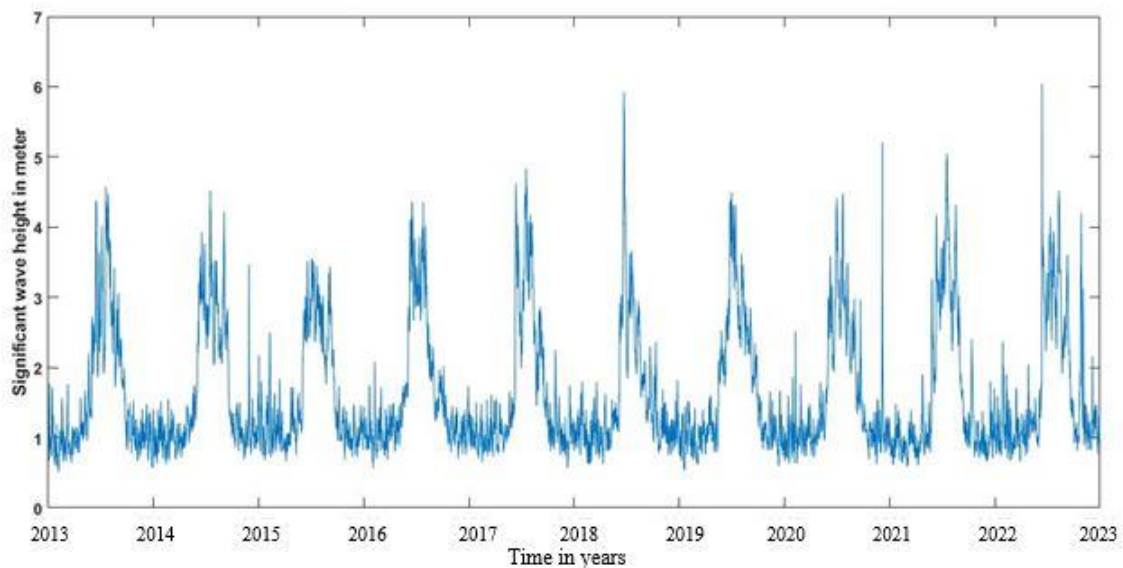


**Fig. 1b.**ERA5 significant wave height of AS (67.1°E, 22.6°N) grid (BIPARJOY) from 2013-2023

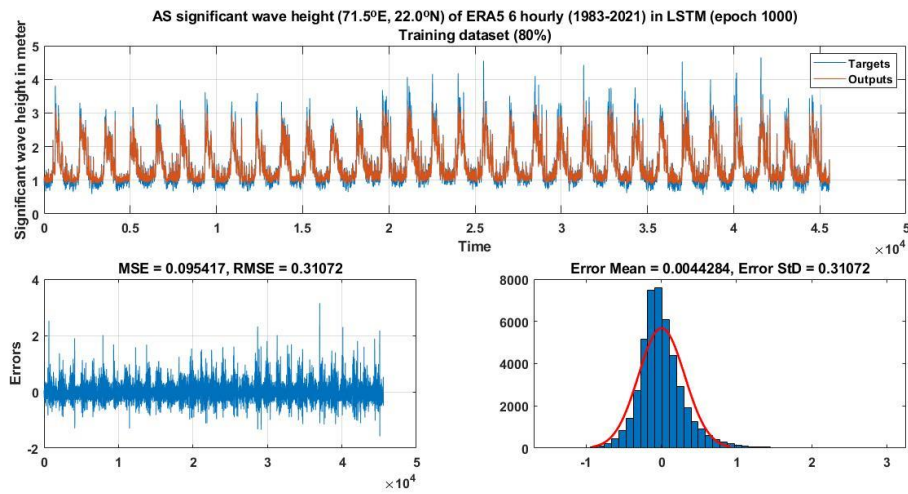


**Fig. 2.** LSTM network applied for AS (71.5°E, 22°N) significant wave height (1983-2021) training dataset

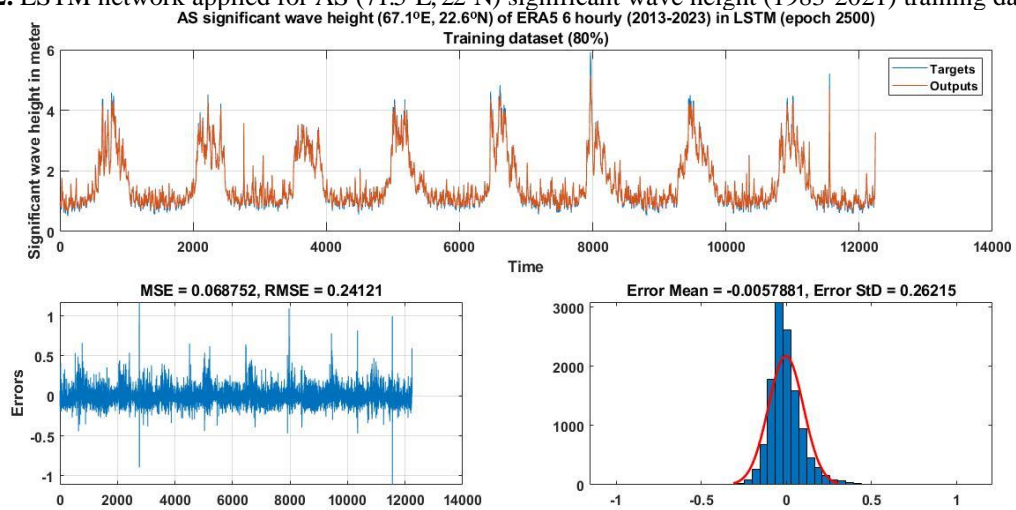


**Fig. 3.** LSTM network applied for AS (67.1°E, 22.6°N) significant wave height (2013-2023) training dataset

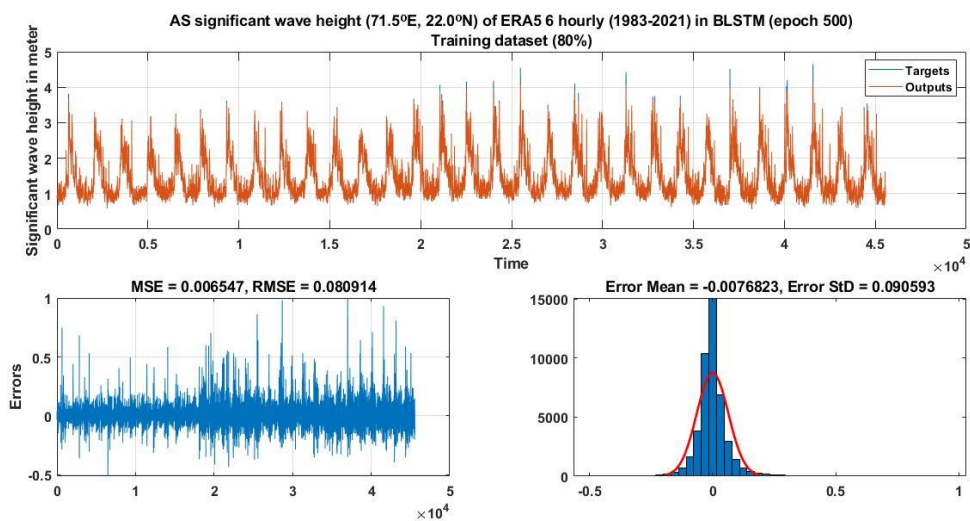


**Fig. 4.** BLSTM network applied for AS (71.5°E, 22°N) significant wave height (1983-2021) training dataset

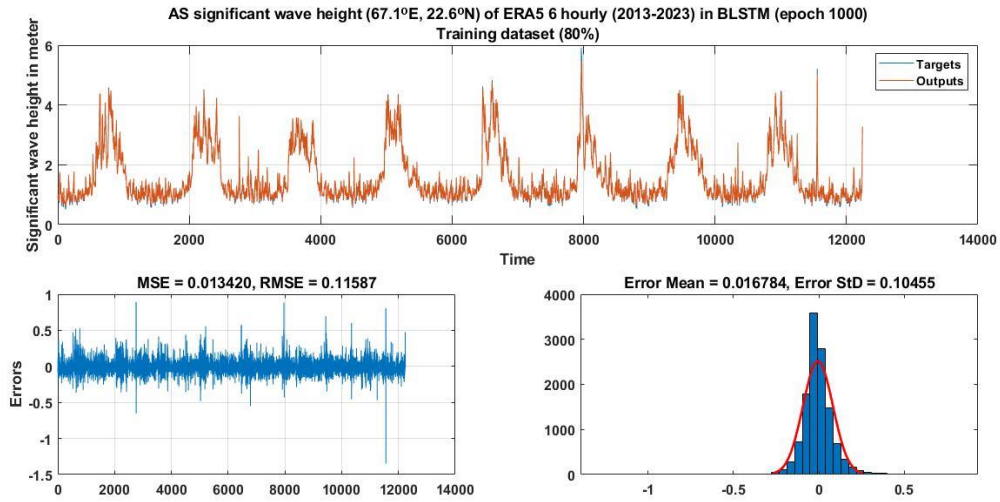


**Fig. 5.**BLSTM network applied for AS (67.5°E, 22.6°N)significant wave height (2013-2023) training dataset

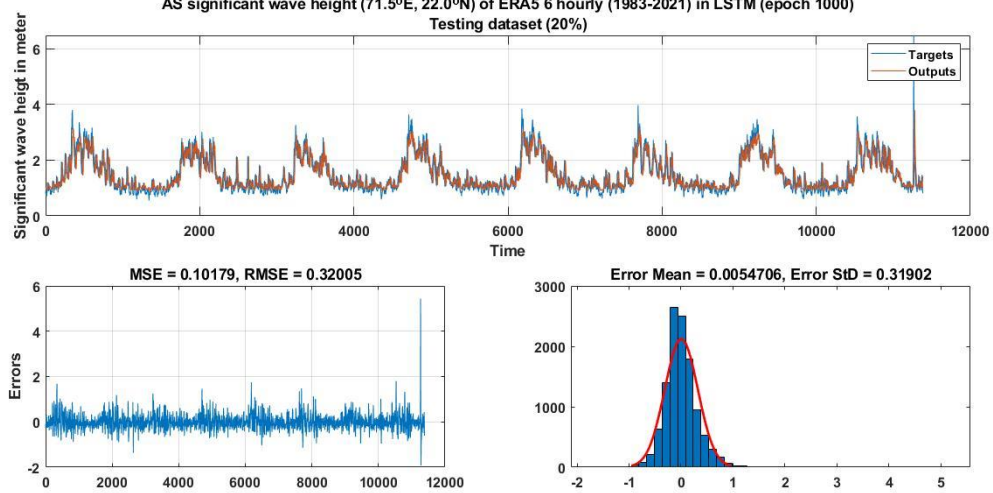


**Fig. 6.**LSTM network applied for AS (71.5°E, 22.0°N)significant wave height (1983-2021) testing dataset

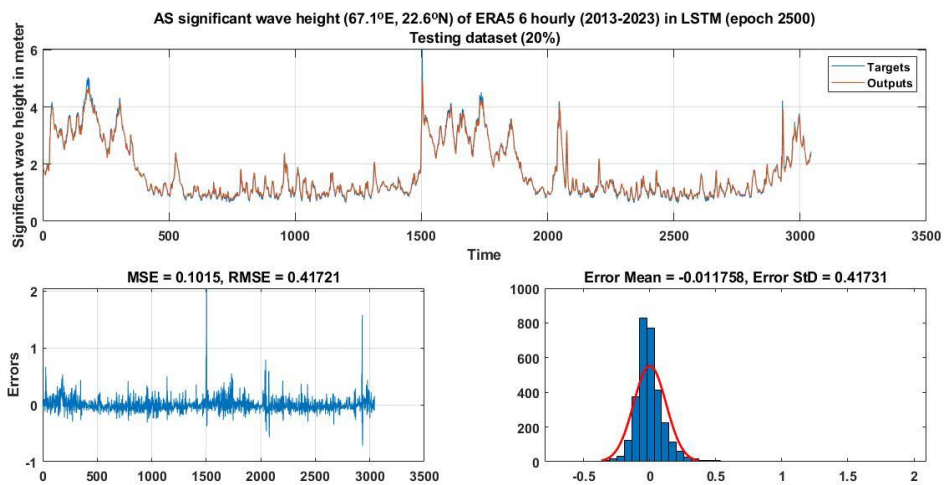


**Fig. 7.**LSTM network applied for AS (67.1°E, 22.6°N)significant wave height (2013-2023) testing dataset

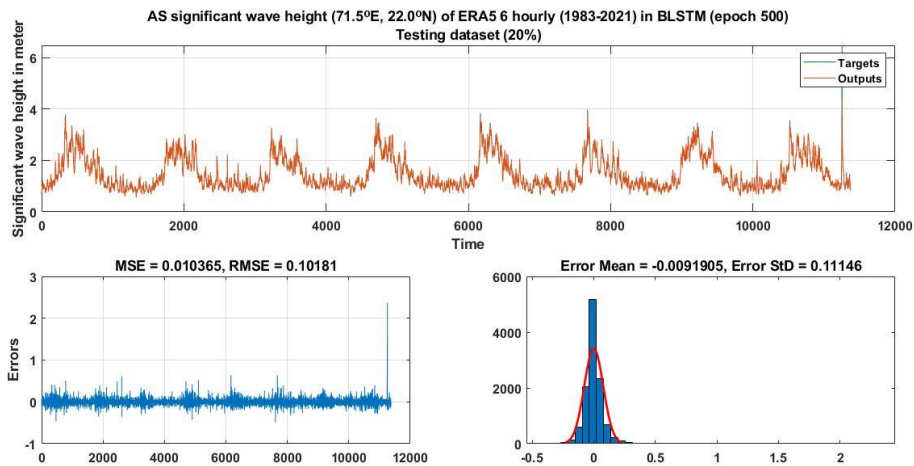


**Fig. 8.**BLSTM network applied for AS (71.5°E, 22°N)significant wave height (1983-2021) testing dataset

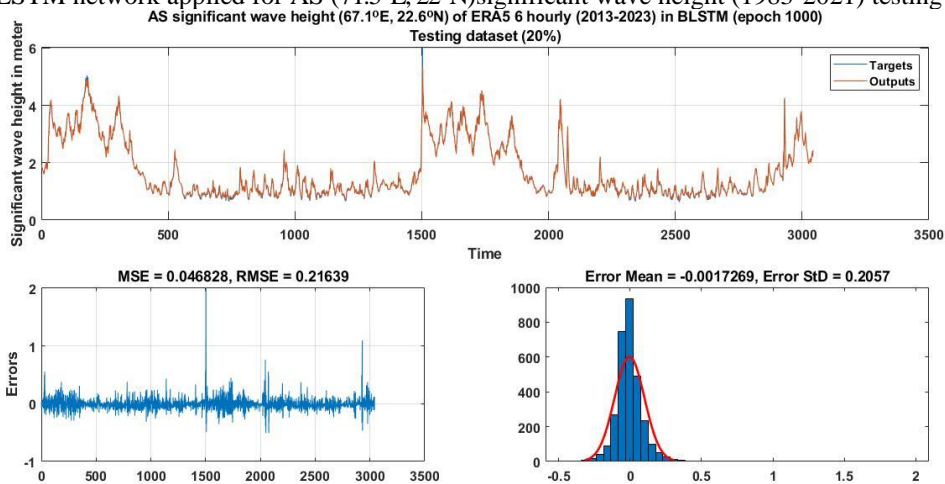


**Fig. 9.**BLSTM network applied for AS (67.1°E, 22.6°N)significant wave height (2013-2023) testing dataset

**Table 1:** RMSE values for LSTM training set

		RMSE			
		AS Grid (71.5°E, 22°N)		AS Grid (67.1°E, 22.6°N)	
Epoch	Hidden Unit	AS (1983-2020)	AS (1983-2021)	AS (2013-2022)	AS (2013-2023)
50	250	0.078658	0.35431	0.13431	0.20983
100	250	0.89459	0.35321	0.12141	0.23422
250	250	0.99765	0.39879	0.21012	0.29912
500	250	0.89999	0.31043	0.10259	0.27999
<b>1000</b>	<b>250</b>	<b>0.073991</b>	<b>0.31072</b>	0.14043	0.23976
<b>2500</b>	<b>250</b>	0.81097	0.31223	<b>0.12085</b>	<b>0.24121</b>

**Table 2:** RMSE values for BLSTM training set

		RMSE			
		AS Grid (71.5°E, 22°N)		AS Grid (67.1°E, 22.6°N)	
Epoch	Hidden Unit	AS (1983-2020)	AS (1983-2021)	AS (2013-2022)	AS (2013-2023)
50	250,250	0.07115	0.06744	0.09325	0.12354
100	250,250	0.06789	0.07123	0.08923	0.81234
250	250,250	0.74321	0.67652	0.98967	0.08234
<b>500</b>	<b>250,250</b>	<b>0.065543</b>	<b>0.08091</b>	0.11011	0.09123
<b>1000</b>	<b>250,250</b>	0.73298	0.81294	<b>0.92791</b>	<b>0.11587</b>
2500	250,250	0.09778	0.07879	0.09989	0.11875

**Table 3:** RMSE values for LSTM testing set



		RMSE			
		AS Grid (71.5°E, 22°N)		AS Grid (67.1°E, 22.6°N)	
Epoch	Hidden Unit	AS (1983-2020)	AS (1983-2021)	AS (2013-2022)	AS (2013-2023)
50	250	0.11194	0.26676	0.10034	0.31011
100	250	0.08432	0.27123	0.12123	0.22321
250	250	0.09897	0.31654	0.11796	0.32169
500	250	0.09123	0.31498	0.16201	0.31982
<b>1000</b>	<b>250</b>	<b>0.08899</b>	<b>0.32005</b>	0.15019	0.34987
<b>2500</b>	<b>250</b>	0.93129	0.33259	<b>0.13541</b>	<b>0.41721</b>

Table 4RMSE values for BLSTM testing set

		RMSE			
		AS Grid (71.5°E, 22°N)		AS Grid (67.1°E, 22.6°N)	
Epoch	Hidden Unit	AS (1983-2020)	AS (1983-2021)	AS (2013-2022)	AS (2013-2023)
50	250,250	0.07559	0.07777	0.11181	0.10999
100	250,250	0.07980	0.08755	0.10789	0.12719
250	250,250	0.08571	0.077291	0.11999	0.22980
<b>500</b>	<b>250,250</b>	<b>0.07480</b>	<b>0.11181</b>	0.10118	0.27623
<b>1000</b>	<b>250,250</b>	0.09943	0.98138	<b>0.10181</b>	<b>0.21639</b>
2500	250,250	0.07587	0.97826	0.13297	0.22686

Table 5RMSE values for BLSTM training set with various lead times

		RMSE			
		AS Grid (71.5°E, 22°N)		AS Grid (67.1°E, 22.6°N)	
Delay	Hidden Units	AS (1983-2020)	AS (1983-2021)	AS (2013-2022)	AS (2013-2023)
		Epoch 1000	Epoch 1000	Epoch 2500	Epoch 2500
<b>1 (6 H)</b>	<b>250,250</b>	0.06554	0.09091	0.09298	0.10879
<b>2 (12 H)</b>	<b>250,250</b>	0.12151	0.11332	0.18441	0.19996
<b>3 (18H)</b>	<b>250,250</b>	0.14658	0.14636	0.20129	0.21983
<b>4 (24H)</b>	<b>250,250</b>	0.17559	0.17897	0.22850	0.22574
<b>8 (48H)</b>	<b>250,250</b>	0.20019	0.26261	0.32608	0.33872
<b>12(72H)</b>	<b>250,250</b>	0.30838	0.31032	0.39162	0.39332

Table 6RMSE values for BLSTM testing set with various lead times

		RMSE			
		AS Grid (71.5°E, 22°N)		AS Grid (67.1°E, 22.6°N)	
Delay	Hidden Units	AS (1983-2020)	AS (1983-2021)	AS (2013-2022)	AS (2013-2023)
		Epoch 1000	Epoch 1000	Epoch 2500	Epoch 2500
<b>1 (6 H)</b>	<b>250,250</b>	0.07280	0.11181	0.10731	0.20639
<b>2 (12 H)</b>	<b>250,250</b>	0.12662	0.13462	0.20642	0.21987
<b>3 (18H)</b>	<b>250,250</b>	0.15404	0.16142	0.22056	0.23376
<b>4 (24H)</b>	<b>250,250</b>	0.18146	0.19363	0.25916	0.26761
<b>8 (48H)</b>	<b>250,250</b>	0.26047	0.27417	0.37525	0.40045
<b>12(72H)</b>	<b>250,250</b>	0.30914	0.31678	0.45496	0.46164

## 5. Conclusions

This research findings uses advanced computer algorithms (deep learning) to predict significant wave height in a specific area (AS) when cyclones hit. A key challenge is how accurate these predictions are for different timeframes (lead durations). Scientists use various error measures like MSE (mean squared error) and RMSE (root mean squared error) to judge how well the predictions match real-world observations. These metrics help them compare different forecasting models objectively. The overall approach combines both in-depth analysis (qualitative investigation) and statistical modelling to make the predictions. By statistically evaluating the forecast quality, researchers can uncover important insights. A low MSE score denotes a good model efficiency. In this research, deep learning models are used to study and describe the details of wave height prediction metrics such as MSE, RMSE, error mean, and error standard. Additionally, comparisons are made between the training and testing errors with lead times for the LSTM and BLSTM models. For the BLSTM model, the error standard is 0.4 and the RMSE is less than 0.5 meter in the event of a 72-hour advance forecast.

To compare the model's output with the intended output in terms of root mean square error, the trial-and-error technique is taken into consideration. The predicted wave height inaccuracy is relatively small in BLSTM models. The results indicate that BLSTM (Bidirectional Long Short-Term Memory) performs better than LSTM (Long Short-Term Memory) at predicting SWH, both during cyclones and calmer periods. This is evident from the figures and tables - BLSTM consistently outperforms LSTM. This suggests that complex deep learning architectures (like BLSTM) could be valuable tools for predicting severe waves in ocean engineering. However, it's important to note that the wave data used in this study wasn't very variable. In the future, researchers will test these deep learning models on data with more complex and dynamic wave patterns, especially those found in harsher environments.

#### **Conflict of Interest:**

On behalf of all authors, the corresponding author states that there is no conflict of interest.

#### **References**

1. Akhil CP, Deka PC (2017) Application of Machine Learning Techniques in Wave Height Forecasting in Marine Environment-A Review. *IJIRESET* 6(5).<http://www.ijirset.com/volume-6-issue-5.html>
2. Ali M, Prasad R (2019) Significant wave height forecasting via an extreme learning machine model integrated with improved complete ensemble empirical mode decomposition. *Renewable and Sustainable Energy Reviews* 104:281-295. <https://doi.org/10.1016/j.rser.2019.01.014>
3. Bethel BJ, Sun W, Dong C, Wang D (2022) Forecasting hurricane-forced significant wave heights using a long short-term memory network in the Caribbean Sea. *Ocean Science* 18:419–436. <https://doi.org/10.5194/os-18-419-2022>
4. Biswas S, Sinha M (2021) Performances of deep learning models for Indian Ocean wind speed prediction. *Modeling Earth Systems and Environment* 7(2):809-831.<https://doi.org/10.1007/s40808-020-00974-9>
5. Deo MC, Jha A, Chaphekar AS, Ravikant K (2001) Neural networks for wave forecasting. *Ocean Engineering* 28:889-898.[https://doi.org/10.1016/S0029-8018\(00\)00027-5](https://doi.org/10.1016/S0029-8018(00)00027-5)
6. Deo M, Naidu CS (1999) Real time wave forecasting using neural networks. *Ocean Engineering* 26:191-203. [https://doi.org/10.1016/S0029-8018\(97\)10025-7](https://doi.org/10.1016/S0029-8018(97)10025-7)
7. Filik UB, Filik T (2017) Wind Speed Prediction Using Artificial Neural Networks Based on Multiple Local Measurements in Eskisehir. *Energy Procedia* 107:264-269.
8. doi: 10.1016/j.egypro.2016.12.147
9. Gopinatha DI, Dwarakishb S (2015) Wave prediction using neural networks at New Mangalore Port along west coast of India. *Aquatic Procedia* 4:143–150.doi: 10.1016/j.aqpro.2015.02.020
10. Graves A, Mohamed AR, Hinton G (2013) Speech recognition with deep recurrent neural networks. *IEEE international conference on acoustics, speech and signal processing*, pp 6645-6649. DOI: 10.1109/ICASSP.2013.6638947
11. Greff K, Srivastava RK, Koutnik J, Steunebrink BR, Schmidhuber J (2017) LSTM: A Search Space Odyssey.[arXiv:1503.04069v2](https://arxiv.org/abs/1503.04069v2) [cs.NE]
12. Hochreiter S, Schmidhuber J (1997) LONG SHORT-TERM MEMORY. *Neural Computation* 9(8):1735-1780.<https://doi.org/10.1162/neco.1997.9.8.1735>
13. Kim J, Moon N (2019)BiLSTM model based on multivariate time series data in multiple field for forecasting trading area. *Journal of Ambient Intelligence and Humanized Computing*.<https://doi.org/10.1007/s12652-019-01398-9>
14. Kumar VS, Mandal S, Kumar SA (2003) Estimation of wind speed and wave height during cyclones. *Ocean Engineering* 30:2239-2253.doi:10.1016/S0029-8018(03)00076-3
15. Liu Y, Sun W, Durlofsky LJ (2019) A Deep-Learning-Based Geological Parameterization for History Matching Complex Models. *Mathematical Geoscience* 51:725-766. <https://doi.org/10.1007/s11004-019-09794-9>
16. Makarynskyy O, Pires-Silva AA, Makarynska D, Ventura-Soares C (2005) Artificial neural networks in wave predictions at the west coast of Portugal. *Computers and Geosciences* 31:415-424. <https://doi.org/10.1016/j.cageo.2004.10.005>
17. M Alif Rizal Yonanta, Didit A, Nugrahinggil S (2018) Wind Wave Prediction by using Autoregressive Integrated Moving Average model : Case Study in Jakarta Bay. *International Journal on ICT* 4(2):33-42. doi:10.21108/indoic.2018.42.300
18. Namini SS, Tavakoli N, Namin AS (2018) A Comparison of ARIMA and LSTM in Forecasting Time Series. 17th IEEE International Conference on Machine Learning and Applications (ICMLA), Orlando, FL, pp. 1394-1401.doi: 10.1109/ICMLA.2018.00227
19. Ni C, Ma X, Wang J (2019) Integrated deep learning model for predicting electrical power generation from wave energy converter. *Proceedings of the 25th International conference on Automation and Computing*, Lancaster University. DOI:10.23919/IConAC.2019.8895237
20. Oh J, Suh KD (2018) Real-time forecasting of wave heights using EOF – wavelet – neural network hybrid model. *Ocean engineering* 150:48-59.

21. <https://doi.org/10.1016/j.oceaneng.2017.12.044>
22. Patel M, Patel A, Ghosh R (2018) Precipitation Nowcasting: Leveraging bidirectional LSTM and 1D CNN. arXiv:1810.10485 (cs)
23. Petitjeana P, Ingladac J, Gancarskia P (2014) Assessing the quality of temporal high-resolution classifications with low-resolution satellite image time series. *International Journal of Remote Sensing*. 35(7)2:693–2712. <http://dx.doi.org/10.1080/01431161.2014.883092>
24. Reddy DS, Prasad PRC (2018) Prediction of vegetation dynamics using NDVI time series data and LSTM. *Modeling Earth Systems and Environment* 4:409-419. <https://doi.org/10.1007/s40808-018-0431-3>
25. Samanta B, Bandoopathyay S, Ganguli R (2006) Comparative Evaluation of Neural Network Learning Algorithms for Ore Grade Estimation. *Mathematical Geology* 38(2). DOI: 10.1007/s11004-005-9010-z
26. Sanil KV, Amrutha MM (2017) Characteristics of high monsoon wind-waves observed at multiple stations in the eastern Arabian Sea. *Ocean Science Discussions*. <https://doi.org/10.5194/os-2017-84>
27. Scott C Jamesa, YushanZhangb, FearghalO'Donnchac (2017) A Machine Learning Framework to Forecast Wave Conditions. arXiv:1709.08725v1
28. Siami-Namini S, Tavakoli N, NaminAS(2019) The Performance of LSTM and BiLSTM in Forecasting Time Series. *IEEE International Conference on Big Data*, pp. 3285-3292. doi:10.1109/BigData47090.2019.9005997
29. Singh OP, Khan TMA, Sazedur Rahman Md (2001) Has the frequency of intense tropical cyclones increased in the north Indian Ocean? *Current Science* 80(4):575–580. doi: 10.1016/j.neunet.2005.06.042
30. Srinivasan R, Abhigna P, Jerrita S, Rajendra V (2016) Analysis of recurrent neural networks for prediction of wave height using wind data. *International Conference on Emerging Trend in Engineering Research at Vels University, Chennai*.
31. SWAMP Group: Allender JH, Barnett TP, Bertotti L, Bruinsma J, Cardone VJ, Cavaleri L, Ephraums J, Golding B, Greenwood A, Guddal J, Günther H, Hasselmann K, Hasselmann S, Joseph P, Kawai S, Komen GJ, Lawson L, Linné H, Long RB, Lybanon M, Maeland E, Rosenthal W, Toba Y, Uji T, de Voogt WJP (1985) Sea wave modeling project (SWAMP), An intercomparison study of wind wave predictions models, part 1: Principal results and conclusions. *Ocean Wave Modeling*, Plenum, pp. 256.
32. Tolman H (1991) A third-generation model for wind waves on slowly varying, unsteady, and inhomogeneous depths and currents. *Journal of Physical Oceanography* 21(6):782-797.
33. Wu T, Cao Y, Wu Z et al (2019) Deep learning for inversion of significant wave height based on actual sea surface backscattering coefficient model. *Multimedia Tools and Applications*. <https://doi.org/10.1007/s11042-019-07967-6>
34. Yulitaa IN, Fananya MI, Arymuthya AM (2017) Bi-directional Long Short-Term Memory using Quantized data of Deep Belief Networks for Sleep Stage Classification. *Procedia Computer Science* 116:530-538. <https://doi.org/10.1016/j.procs.2017.10.042>
35. Zhang L, Oey L (2019) An observational analysis of ocean surface waves in tropical cyclones in the western North Pacific Ocean. *Journal of Geophysical Research: Oceans* 124:184-195. <https://doi.org/10.1029/2018JC014517>
36. Zhuxin O, Yaoting G, Xuefeng Z, Xiangyu Wu, Dianjun Z(2024) Significant Wave Height Forecasting Based on EMD-TimesNet Networks., *J. Mar. Sci. Eng.* 12(4), 536. <https://doi.org/10.3390/jmse12040536>

#### Appendix A: Deep learning Algorithms (LSTM and BLSTM)

Input: Timeseries significant wave height (swh) data

Outputs: MSE and RMSE values of the forecasted swh data

% Set input delay

delay ← [1]

% Divide data into:

% 80% training and 20% testing of significant wave height data

Size long(swh\_data) \*0.80

Training ← swh\_data

Testing ← swh\_data

% Input time series

swh\_data ← read Input from excel File;

% eliminating NaN value and normalizeswh\_data

swh\_data ← swh\_datacreation (swh\_data, option);

% split data into testing and training data

swh\_data ← swh\_datadivision (swh\_data, option);

% create delay for time series

swh\_data ← preparation of Time Series swh\_data (LSTMInput (swh\_data, option));

% Define LSTM model

option ← LSTMArchitect (option);

% Standardize input of significant wave height swh\_data and eliminatingNaN

```
swh_data ← data creation (input, option)
% ---- swh_datacreation ----
if option. is normalized
fori=1: size (swh_data. Varr,1)
swh_data.mu (1, i) ← mean (swh_data. Varr (i, :),'omitna');
swh_data. sigma (1, i) ← std (swh_data. Varr (i, :),'omitna');
swh_data. Varr (i, :) ← (swh_data. Varr (i, :) - data.mu (1, i)). / data. sigma (1, i);
end
% de-Normalizing of swh_data
function x ← deNormalize_swh_Data (x, swh_data);
x ← x*swh_data.sig+swh_data.mu;
% make some delays on input file
option. isUseDelays
    Delays = option. Delays;
MaxDelay = max (Delays);
    Range = MaxDelay+1: T;
% BiLSTM Deep learning Architect
Option. layers ← [ sequenceInputLayer (input Size),
BilstmLayer(numHidden_Units1,'Output_Mode','sequence')
BilstmLayer (numHidden_Units2,'Output_Mode','last')
FullyConnectedLayer(num_Responses)
RegressionLayer];
%Training Network Options
opts ← training Opts ('adam', 'Max Epochs', max Epochs, 'GradientThreshold', 'InitialLearnRate', 'Learn Rate
Schedule','piecewise', 'LearnRateDropPeriod', 'LearnRateDropFactor', 'Verbose', 'MiniBatchSize', miniBatchSize,
'ExecutionEnvironment', executionEnvironment, 'Plots', trainingProgress);
% ---- Assess LSTM network ----
Function_results ← Evaluate Net (results, swh_data, option)
% denormalizingswh_data
if option. isNormalize_swh_Data
    Training Outputs ← deNormalize_swh_Data (Train Outputs, swh_data);
    Testing Outputs ← deNormalize_swh_Data (Test Outputs, swh_data);
End
% print Results
function Plot Results (Training Outputs, Testing Output, Regression Output)
    Errors ← Target - Output;
    MSE ← mean (Error. ^2);
    RMSE ← sqrt (MSE);
End
```